Title: A global analysis of subsidence, relative sea-level change and coastal flood exposure

Authors:

Robert J. Nicholls[1], Daniel Lincke[2], Jochen Hinkel[2,3], Sally Brown[4], Athanasios T. Vafeidis[5], Benoit Meyssignac[6], Susan E. Hanson[7], Jan Merkens[5], Jiayi Fang[8]

Affiliations:

[1] Tyndall Centre for Climate Change Research, University of East Anglia, Norwich, UK

[2] Global Climate Forum e.V. (GCF), Berlin, Germany

[3] Division of Resource Economics, Albrecht Daniel Thaer-Institute and Berlin Workshop in Institutional Analysis of Social-Ecological Systems (WINS), Humboldt-University, Berlin, Germany

[4] Department of Life and Environmental Sciences, Faculty of Science and Technology, Bournemouth University, UK

[5] Kiel University, Department of Geography, Kiel, Germany

[6] LEGOS, Université de Toulouse, CNES, CNRS, UPS, IRD, 31400 Toulouse, France.

[7] School of Engineering, University of Southampton, Southampton, UK

[8] School of Geographic Sciences, East China Normal University, Shanghai, 200241, China

ORCID

Robert J. Nicholls 0000-0002-9715-1109

Daniel Lincke 0000-0003-4250-5077

Jochen Hinkel	0000-0001-7590-992X
Sally Brown	0000-0003-1185-1962
Athanasios T. Vafeidis	0000-0002-3906-5544
Benoit Meyssignac	0000-0001-6325-9843
Susan E. Hanson	0000-0002-2198-1595
Jan Merkens	0000-0003-0916-2906
Jiayi Fang	0000-0002-0420-5615

Editors Summary:

Land subsidence/uplift influences the rate of sea-level rise. Most coastal populations live in subsiding areas and as a result experience average rates of relative sea-level rise three to four times faster than due to climate change alone. This indicates the need for policy to address subsidence.

Abstract:

Climate-induced sea-level rise and vertical land movements, including natural and human-induced subsidence in sedimentary coastal lowlands, combine to change relative sea levels around the world's coast. Although this affects local rates of sea-level rise, assessments of the coastal impacts of subsidence are lacking on a global scale. Here, we quantify global-mean relative sea-level rise to be 2.5 mm/yr over the last two decades. However, as coastal inhabitants are preferentially located in subsiding locations, they experience an average relative sea-level rise up to four times faster at 7.8 to 9.9 mm/yr. These results indicate that the impacts and adaptation needs are much higher than reported global sea-level rise measurements suggest. In particular, human-induced subsidence in and surrounding coastal cities can be rapidly reduced with appropriate policy for groundwater utilization and drainage. Such policy would offer substantial and rapid benefits to reduce growth of coastal flood exposure due to relative sea-level rise.

Main Text:

It is widely recognised that climate-induced sea-level rise (SLR) is raising water levels around the world's coast[1-3] and that this will lead to an increase in flood risk and other impacts unless there is corresponding adaptation[4]. Against this background, a large literature has assessed the magnitude of SLR, and its impacts and adaptation needs at global scales[2]. Indeed, this literature is essential for setting and evaluating mitigation targets, strategic adaptation, and designing financial arrangements for funding adaptation and compensation for loss and damage. Over time, this literature has progressed from focusing on climate-induced regional SLR to also including geological sources of local relative sea-level change such as glacial-isostatic adjustment (GIA) in order to serve local adaptation needs, for which the source of relative SLR is irrelevant. To our knowledge, however, no global study has quantitatively considered the contribution of subsidence to global SLR risk. This may constitute a serious limitation in global exposure estimates as human-induced subsidence in particular can lead to rates of local SLR that are much higher than current rates of climate-induced SLR. Furthermore, these high rates occur specifically in densely populated areas such as cities and deltas. This could have a large effect on people's experience of relative sea-level rise, but so far the size of this effect has not been studied at global scales.

Important geological processes that are contributing to relative sea-level change include tectonics, glacial-isostatic adjustment (GIA) and subsidence in geologically recent sedimentary deposits such as deltas, which can be significantly enhanced by human agency especially groundwater withdrawal[5-10]. As global models are available (e.g., Peltier et al[11]) and it is a long-term stable process causing either uplift or subsidence depending on location, GIA is often considered in global analysis of relative sea level and impacts. Other sources of land elevation change are not regularly included, being implicitly seen as a local problem.

Natural subsidence, mainly due to the compaction of young sediments in deltas, is widespread and significant[12]. However, the most rapid rates of subsidence are human-induced. These are caused by accelerated compaction primarily due to withdrawal of underground fluids including groundwater, oil and gas, as well as drainage of organic soils[8,12]. As Ericson et al[13], Syvitski et al[14] and Tessler et al[15] among others have demonstrated, these processes are marked in many of the world's deltas and are often compounded by both local flood defences within the delta and upstream dams, which collectively reduce the sediment supply that maintains these sedimentary landforms. Sand extraction and mining can exacerbate this loss of sediment supply. Cumulatively, human effects on subsidence are at their largest in some coastal cities located on deltas and alluvial plains: a net subsidence of more than 4 m has occurred during the 20th century in parts of Tokyo, and 2 to 3 m in Shanghai, Bangkok, Jakarta and New Orleans[16-19]. Many deltas and subsiding cities are in Asia and the World Bank[20] recognised that subsidence could be as significant as climate-induced SLR in parts of coastal Asia over the 21st century.

To analyse the relative importance of subsidence on relative SLR, we consider data for four components of relative sea-level change: (1) climate-induced sea-level change[21,22]; (2) glacial-isostatic adjustment (GIA)[11]; (3) recent estimates of total deltaic subsidence, including natural and human-induced changes; and (4) recent estimates of human-induced subsidence in coastal cities on deltas and alluvial plains (which operate at a sub-delta scale and hence is additional to the subsidence due to component 3). In addition to the individual components, we also consider the combined effect of all these components, which is the local relative SLR. To compute global relative SLR, we weight local relative SLR values by the length of coast and thus obtain an estimate of the average relative SLR per kilometre of coast. Given that the distribution of coastal population and hence SLR risks and adaptation needs are not uniform, we also estimate the global relative SLR weighted by coastal population, giving an estimate of the average relative SLR per coastal resident. We then consider the relative role of subsidence in enhancing coastal flood risk to 2050 compared to other changes, assuming current estimates of subsidence continue. For this, we focus on the coastal flood plain population (i.e., exposure) as a metric as it is independent of adaptation. All components, data and methods are defined and described in more detail in the Methods.

Considering weighting by coastal length, the analysis shows that contemporary global-mean coastal relative SLR, including climate and geological components, averages 2.5 mm/yr over the last two decades with climate-induced SLR being the dominant component (Fig. 1; Table 1). This is less than the climate-induced change component alone as GIA causes a net average fall in relative sea level around the world's coasts. Globally, the combined effect of subsidence components in deltas and coastal cities is almost negligible and cannot be distinguished in the cumulative distribution curve (Extended Data Fig. 1). This reflects that, based on the data analysed, only 6.5 percent and 0.8 percent of the world's coast comprises subsiding deltas and subsiding cities respectively.

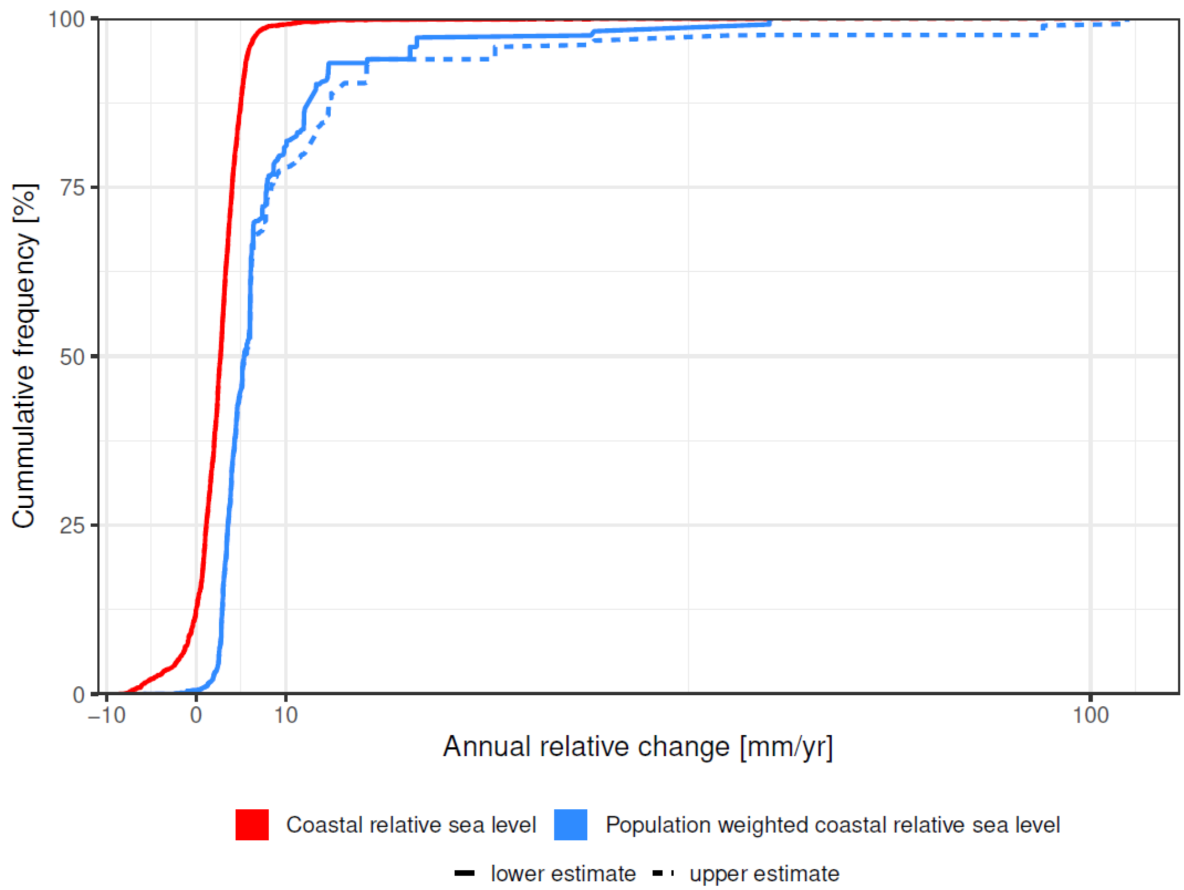

Fig 1: *Cumulative distribution of contemporary (last two decades) length-weighted and population-weighted coastal relative sea-level rise, respectively. This includes lower and upper estimates to express uncertainty, although for length weighting the difference is too small to be distinguished.*

Table 1: Contribution *of the climate and geological components to relative sea−level change for length-weighted and population-weighted cases respectively. Average values are reported, except for cities and the global-mean sum where a low/high range is used to express the uncertainty in subsidence (see Supplementary Table 2).*

Relative SLR component	Contribution to relative sea−level change			
	Length-weighted		Population-weighted	
	mm/yr	%	mm/yr	%
Climate-induced SLR (1993 to 2015)	3.2	122	3.8	39 to 49
Glacial Isostatic Adjustment	-0.8	-32	-0.3	-3
Delta Subsidence	0.1	4	1.6	16 to 21
City Subsidence	0.1	3	2.7 to 4.8	35 to 49
Global−mean sum	2.6		7.8 to 9.9	

In contrast, weighting by coastal population shows that coastal inhabitants on average experienced much higher relative SLR, reflecting the heterogeneous distribution of coastal population (Fig. 1, Table 1). The median relative SLR per person is about 5 mm/yr, while the mean is up to four times higher at 7.8 to 9.9 mm/yr over the last two decades. This global enhancement of average sea-level rise per person mainly reflects that coastal residents are concentrated in subsiding areas including deltas, and especially in subsiding coastal cities, which gives a high-end tail to the distribution (Fig. 1; Extended Data Fig. 1). Effectively, delta and city subsidence and population density are not independent - higher population densities lead to human actions that promote subsidence and loss of elevation. Furthermore, deltas have fertile soils and hence have historically been hotspots for human management and development[14]. Hence, the relative sea-level change components linked to human activities tend to increase with population density around the world’s coasts (Extended Data Fig 2). We estimate that 51 to 70 percent of the total global average relative SLR experienced by people is due to delta and city subsidence (Table 1). In contrast, the global effect of GIA is almost negligible when considering population weighting (Extended Data Fig. 1).

Globally, average sea-level changes over the last two decades are distributed unevenly across coastal length and coastal population (Fig. 1). About 12.5 percent of the world's coast by length is experiencing relative sea-level fall, this being attributed to uplift caused by GIA. However, these areas only have 2.7 million inhabitants (less than one percent of global coastal population). Conversely, only about 0.7-0.8 percent of the world's coast by length is experiencing a SLR above 10 mm/yr (the range covers uncertainty in city subsidence). However, these coasts contain large subsiding cities such as Jakarta and 147 to 171 million inhabitants (19.1-22.3 percent of the global coastal population).

Average coastal population-weighted relative sea-level rise is also often higher at the regional level than coastal-length weighted relative sea-level rise estimates (Fig 2): 11 of 23 world regions show more than 50 percent increases in population-weighted relative sea-level rise when compared to coastal length-weighted relative sea-level rise (Supplementary Table 4). Seven regions have an increase of more than 100 percent (the Baltic Sea Coast, North and West Europe, North America Atlantic Coast, North America Pacific Coast, South America Pacific Coast, Southern Mediterranean and South-East Asia), reflecting regions where coastal residents are strongly concentrated in areas where relative sea-level rise is higher. In absolute terms, the effect in South, South-east and East Asia is noteworthy (Supplementary Table 4), as these regions collectively contain 71% of the global coastal population below 10-m elevation (546 million out of 768 million people globally in 2015) and 75% of the global coastal floodplain population (185 million out of 249 million people globally in 2015).

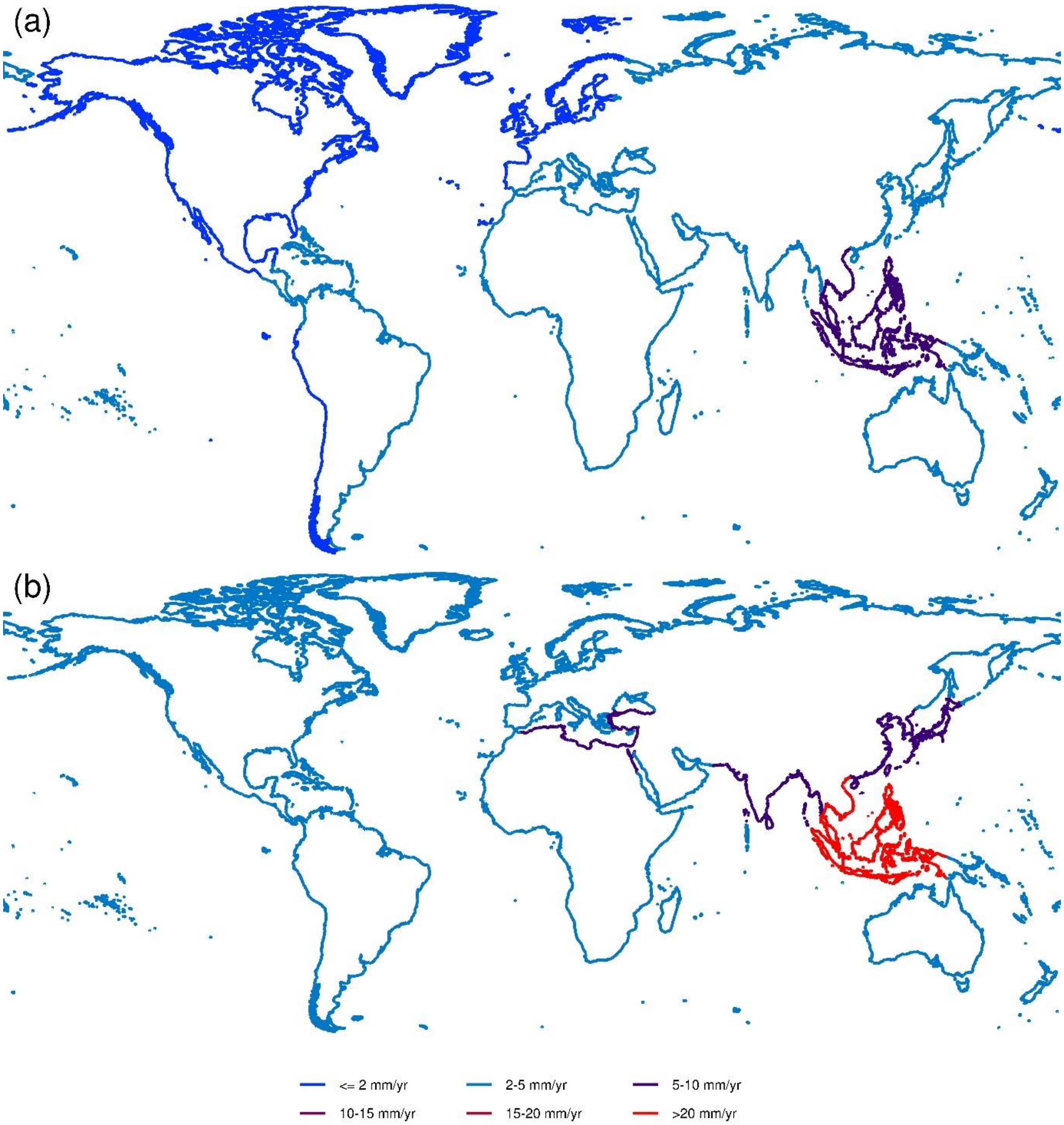

Fig 2: *Average relative sea-level rise for 23 coastal world regions. (a) Length-weighted and (b) population-weighted. (see Supplementary Table 3 for region definitions).*

Finally, we assess the contributions of climate-induced SLR, GIA, delta subsidence and city subsidence to the evolution of the global population living in the coastal flood plain from 2015 to 2050 (Fig. 3). This assumes that the observed subsidence in deltas and cities continues to 2050, representing a plausible scenario of future subsidence. In 2015, this flood plain population is approximately 235 million people. Assuming no subsidence and no climate-induced SLR, this population rises to about 280 million people by 2050 due to socio-economic development alone (here SSP2)[23]. Adding the GIA component, reduces this number to 270 million, while adding the delta subsidence component increases it back to about 280 million people. Adding the uncontrolled city subsidence component further increases the flood plain population to about 305 to 320 million people (a net increase of 25 to 40 million people summing across the GIA, delta and city subsidence components). Additionally considering climate-induced SLR, the exposed population increases to 330 to 350 million by 2050 (a net increase of 25 to 30 million people due to climate change) (Fig. 3(d)). The effects of subsidence and climate-induced SLR on exposed population numbers can therefore be seen as being comparable in magnitude over the next 30 years. Under other SSPs, the results are similar (see Extended Data Fig, 3).

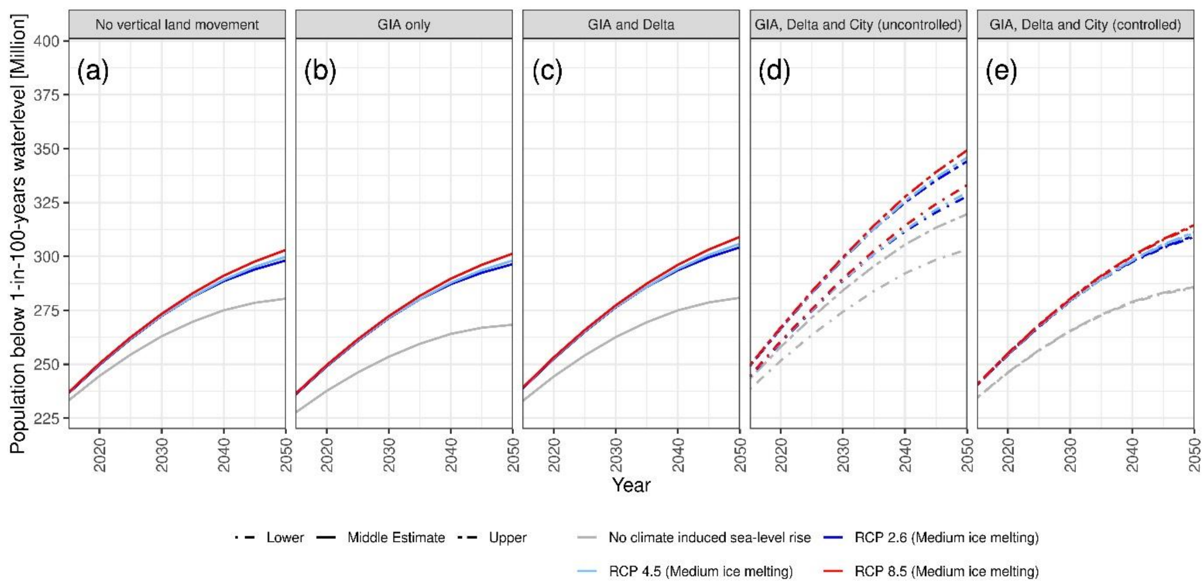

Fig 3: *Global population in the coastal flood plain from 2015 to 2050. This considers sea-level rise scenarios under RCP2.6, RCP4.5 and RCP8.5 emissions, as well as no climate-induced sea-level rise as a reference, and assumes the SSP2 socio-economic scenario. Subsidence/GIA assumptions as indicated. (a) No vertical land movement. (b) GIA only. (c) GIA and delta subsidence. (d) GIA, delta and uncontrolled city subsidence. (e) GIA, delta and city subsidence controlled to 5 mm/yr. The uncertainty bands reflect uncertainty in rates of city subsidence (see Fig. 1). Simulations start in 1995, while the flood plain is defined based on the 100-year event.*

These findings have important implications for coastal management, climate action and sustainability goals. For climate mitigation, they mean that contemporary and future global SLR risks and adaptation needs are much higher than previously assessed. For adaptation, this means that reducing human-induced subsidence constitutes a globally significant coastal adaptation option. While from a conceptual point of view it can be debated if managing subsidence constitutes adaptation, from a practical point of view this has a higher potential for reducing coastal exposure than climate mitigation over the next 30 years. For example, if we reduce coastal city subsidence to 5 mm/yr, population exposure could be reduced by about 20 to 35 million people or 6 to 10 percent by 2050 compared with unreduced city subsidence (Fig. 3e compared to Fig. 3d), whereas under ambitious climate mitigation (i.e., from RCP8.5 to RCP2.6), population exposure would be reduced by about 5 million people or 1.5 percent over the same timeframe. Climate mitigation would lead to much larger benefits after 2050[2,24] (not assessed here), and these two policies can and should be complementary. Reducing city subsidence to 5 mm/yr or less is feasible as demonstrated in the Netherlands and many Asian cities (e.g., Tokyo, Osaka, Shanghai), where it involves managing groundwater withdrawal and maintaining high water tables. However, these policies generally reduce rather than stop all subsidence[9,17] and there are wider implications and risks associated with rising water tables for cities. Therefore, while some subsidence control may be feasible, other SLR adaptation approaches will still be necessary and compatible with adapting to climate change[2,18]. Controlled flooding and sedimentation could be an innovative response to loss of elevation in deltas, especially in agricultural areas. This would involve a major shift in thinking in delta management to controlling rather than eliminating flooding, and recognising sediment and sedimentation as a resource[14,25,26].

The influence of subsidence on relative SLR has grown through the 20th century alongside expanding coastal populations in susceptible areas – notably in deltas and especially in large and expanding cities on those deltas. The results discussed here indicate this will certainly continue and maybe even grow in magnitude and extent with increasing coastal urbanisation in susceptible settings. Improved measurements of natural and human-induced subsidence processes are emerging and analysed systematically, as shown here, this will allow fuller appreciation of the potential consequences of relative SLR at regional to global scales and appropriate responses developed[27-29].

In conclusion, this analysis shows that, due to its coincidence with major population centres, subsidence has global social and economic implications. Its influence on exposure to coastal flooding is comparable to, if not greater than, climate-induced sea-level rise over the next few decades and will remain significant thereafter. As such, subsidence should be better recognized in regional and global assessments of relative sea-level rise impacts, and not simply restricted to local assessments. This, in turn, would improve the evidential basis for adaptation, disaster risk reduction, and development strategies in coastal areas.

References:

1 Nerem, R. S. *et al.* Climate-change–driven accelerated sea-level rise detected in the altimeter era. *Proceedings of the National Academy of Sciences* **115**, 2022, https://doi.org/10.1073/pnas.1717312115 (2018).

2 Oppenheimer, M. *et al.* in *IPCC Special Report on the Ocean and Cryosphere in a Changing Climate* (eds H O Pörtner *et al.*) Ch. 4 Sea level rise and implications for low lying islands, coasts and communities, (Intergovernmental Panel on Climate Change (IPCC), 2019)

3 Church, J. A. *et al.* in *Climate Change 2013: The Physical Science Basis. Contribution of Working Group I to the Fifth Assessment Report of the Intergovernmental Panel on Climate Change* (eds T F Stocker *et al.*) Ch. 13 Sea level change, 1137-1216 (Cambridge University Press, 2013)

4 Wong, P. P. *et al.* in *Climate Change 2014: Impacts, Adaptation, and Vulnerability, Pt A: Global and Sectoral Aspects: Working Group II Contribution to the Fifth Assessment Report of the Intergovernmental Panel on Climate Change* (eds C. B. Field *et al.*) Ch. 5 Coastal systems and low-lying areas, 361-409 (2014)

5 Emery, K. O. & Aubrey, D. G. *Sea Levels, Land Levels, and Tide Gauges*. (Springer-Verlag, 1991).

6 Rovere, A., Stocchi, P. & Vacchi, M. Eustatic and relative sea level changes. *Current Climate Change Reports* **2**, 221-231, https://doi.org/10.1007/s40641-016-0045-7 (2016).

7 Lickley, M. J., Hay, C. C., Tamisiea, M. E. & Mitrovica, J. X. Bias in estimates of global mean sea level change inferred from satellite altimetry. *Journal of Climate* **31**, 5263-5271, https://doi.org/10.1175/JCLI-D-18-0024.1 (2018).

8 Milliman, J. & Haq, B. U.(eds) *Sea-Level Rise and Coastal Subsidence: Causes, Consequences, and Strategies*. (Springer, 1996).

9 Erkens, G., Bucx, T., Dam, R., de Lange, G. & Lambert, J. Sinking coastal cities. *Proc. IAHS* **372**, 189-198, https://doi.org/10.5194/piahs-372-189-2015 (2015).

10 Frederikse, T., Riva, R. E. M. & King, M. A. Ocean bottom deformation due to present-day mass redistribution and its impact on sea level observations. *Geophysical Research Letters* **44**, 12,306-312,314, https://doi.org/10.1002/2017GL075419 (2017).

11 Peltier, W. R., Argus, D. F. & Drummond, R. Space geodesy constrains ice age terminal deglaciation: The global ICE-6G_C (VM5a) model. *Journal of Geophysical Research: Solid Earth* **120**, 450-487, https://doi.org/10.1002/2014JB011176 (2015).

12 Syvitski, J. P. M. Deltas at risk. *Sustainability Science* **3**, 23-32, https://doi.org/10.1007/s11625-008-0043-3 (2008).

13 Ericson, J. P., Vörösmarty, C. J., Dingman, S. L., Ward, L. G. & Meybeck, M. Effective sea-level rise and deltas: Causes of change and human dimension implications. *Global and Planetary Change* **50**, 63-82, https://doi.org/10.1016/j.gloplacha.2005.07.004 (2006).

14 Syvitski, J. P. M. *et al.* Sinking deltas due to human activities. *Nature Geoscience* **2**, 681-686, https://doi.org/10.1038/ngeo629 (2009).

15 Tessler, Z. D., Vörösmarty, C. J., Overeem, I. & Syvitski, J. P. M. A model of water and sediment balance as determinants of relative sea level rise in contemporary and future deltas. *Geomorphology* **305**, 209-220, https://doi.org/10.1016/j.geomorph.2017.09.040 (2018).

16 Nicholls, R. J. Coastal megacities and climate change. *GeoJournal* **37**, 369-379, https://doi.org/10.1007/BF00814018 (1995).

17 Kaneko, S. & Toyota, T. in *Groundwater and Subsurface Environments: Human Impacts in Asian Coastal Cities* (ed Makoto Taniguchi) Ch. Long-term urbanization and land subsidence in Asian megacities: An indicators system approach, 249-270 (Springer Japan, 2011) https://doi.org/10.1007/978-4-431-53904-9_13

18 Esteban, M. *et al.* Adaptation to sea level rise: Learning from present examples of land subsidence. *Ocean & Coastal Management* **189**, 104852, https://doi.org/10.1016/j.ocecoaman.2019.104852 (2020).

19 Burkett, V. B., Zilkowski, D. B. & Hart, D. A. in *Proceedings of USGS Aquifer Mechanics and Subsidence Interest Group conference, Galveston, TX, USA 27–29 November 2001. USGS water resources division open-file report series 03-308* (eds K R Prince & D. L. Galloway) Ch. Sea level rise and subsidence: implications for flooding in New Orleans, Louisiana, 63-70 (US Geological Survey, 2003)

20 World Bank. Climate risks and adaptation in Asian coastal megacities: A synthesis report. 97pp (World Bank, Washington DC, USA, 2010)

21 Ablain, M. *et al.* Improved sea level record over the satellite altimetry era (1993–2010) from the Climate Change Initiative project. *Ocean Science* **11**, 67-82, https://doi.org/10.5194/os-11-67-2015 (2015).

22 Legeais, J. F. *et al.* An improved and homogeneous altimeter sea level record from the ESA Climate Change Initiative. *Earth Systems Scientific Data* **10**, 281-301, https://doi.org/10.5194/essd-10-281-2018 (2018).

23 Kriegler, E. *et al.* A new scenario framework for climate change research: the concept of shared climate policy assumptions. *Climatic Change* **122**, 401-414, https://doi.org/10.1007/s10584-013-0971-5 (2014).

24 Nicholls, R. J. *et al.* Stabilization of global temperature at 1.5°C and 2.0°C: implications for coastal areas. *Philosophical Transactions of the Royal Society A: Mathematical, Physical and Engineering Sciences* **376**, 20160448, https://doi.org/10.1098/rsta.2016.0448 (2018).

25 Day, J. W. *et al.* Restoration of the Mississippi Delta: Lessons from Hurricanes Katrina and Rita. *Science* **315**, 1679, https://doi.org/10.1126/science.1137030 (2007).

26 Darby, S. E., Appeaning Addo, K., Hazra, S., Rahman, M. M. & Nicholls, R. J. in *Deltas in the Anthropocene* (eds Robert J. Nicholls, W. Neil Adger, Craig W. Hutton, & Susan E. Hanson) Ch. 5 Fluvial sediment supply and relative sea-level rise, 103-126 (Springer International Publishing, 2020) https://doi.org/10.1007/978-3-030-23517-8_5

27 Nicholls, R. J. *et al.* Sea-level scenarios for evaluating coastal impacts. *WIREs Climate Change* **5**, 129-150, https://doi.org/10.1002/wcc.253 (2014).

28 Erkens, G. & Sutanudjaja, E. H. Towards a global land subsidence map. *Proc. IAHS* **372**, 83-87, https://doi.org/10.5194/piahs-372-83-2015 (2015).

29 Higgins, S. A. Review: Advances in delta-subsidence research using satellite methods. *Hydrogeology Journal* **24**, 587-600, https://doi.org/10.1007/s10040-015-1330-6 (2016).

Methods:

The analysis uses the framework of the Dynamic Interactive Vulnerability Assessment (DIVA) model which has been applied to problems such as coastal erosion[30], coastal flooding[31] and coastal wetland change[32], among others. The underlying structure is a dataset of coastal areas and floodplains based on 12,148 coastal segments which divide the world's coast (excluding Antarctica) into lengths of similar coastal characteristics[33]. The segments are variable in length with average of 70 km. All data such as sea-level rise (SLR), socio-economic development, extreme water levels, subsidence rates, etc., is associated with the appropriate segment.

To analyse the global effects of subsidence on relative sea-level rise we combine data on four components of relative sea-level change:

1. Satellite observations of sea-level change from 1993 to 2015;
2. Glacial-isostatic adjustment (GIA), derived from the model of Peltier et al[11];
3. Delta subsidence, which includes natural and anthropogenic subsidence in 117 deltas worldwide, building on the earlier work of Ericson et al[13];
4. City subsidence, which captures the additional subsidence beyond delta subsidence that coastal cities in deltaic and alluvial plains experience. We thereby consider susceptible coastal cities with populations exceeding one million people in 2005 that are prone to subsidence (following Nicholls et al[34]).

These four components are independent and hence can simply be summed for each segment. We exclude uplift and subsidence due to due to other processes such as tectonics[6] as there are no consistent global datasets available. Most analysis of these processes are local or regional (e.g., National Research Council[35]) and obtaining the data required to create relative sea-level rise scenarios at the global scale is problematic[27]. The few studies that systematically analyse data on vertical land movements globally using measurements at tide gauges[36,37] find that GIA (already included in the analysis) explains a large part of the observed trends.

The major limitation in the analysis is that subsiding cities with less than one million are excluded, again reflecting a lack of consistent data at the global scale. This means that our estimates of the effect of city subsidence on relative SLR are minimum estimates.

For assessing the effects of future climate-induced SLR we use the same scenarios as Hinkel et al[31] For delta and city subsidence from 2015 to 2050, we assume that the observed rates of subsidence continue at the same rate. It is recognised that these rates may be subject to significant change, especially those due to human influence (e.g., Phien-wej et al[38]). Hence, they should be considered as indicative scenarios rather than projections. The purpose of the analysis is to estimate the relative magnitudes of these processes rather than create projections.

For present and future population we use the scenarios of Merkens et al[39].

Data:

The following datasets are used in this analysis.

Sea-level change

For the sea-level change observations, we use the satellite altimetry product from the European Space Agency (ESA) Climate Change Initiative sea level (CCI_SL) project. We use this product because the data is computed with consistent geophysical corrections throughout the whole records and is thus specifically tailored for trend estimates[21,22]. The product is a 2-D gridded sea surface height of delayed time anomalies described and validated in Legeais et al[22]. The product is freely available on http://www.esa-sealevel-cci.org/products. We analysed the data over the period 1993 to 2015. The dataset is provided at monthly intervals on a ¼° regular grid as anomalies computed with reference to the 1993-2012 period. Sea-level anomalies for the study sites were extracted from the global dataset. At high latitude (>82°), satellite altimetry data is not available (because of the inclination of the satellites). Close to the coast, data is available until 15km from the coast. However, at 15 km from the coast some significant errors can arise in geophysical corrections applied to the sea level estimate. These errors arise from land contamination in the satellite radiometer measurement which is used for the wet-tropospheric correction, or in the radar measurement which is used to estimate the altimetry range or in geophysical models such as tide models (because of inaccurate bathymetry for example). To remove this potential spurious data we discarded all data at less than 25 km from the coast. To ensure that all spurious data was removed we checked that the difference between the data close to the coast and adjacent data offshore was within the typical sea level variability range (following The Climate Change Initiative Coastal Sea Level Team[40]). For the trend estimate, we used a least square fit that estimate at the same time the annual cycle, the semi-annual cycle and the trend. The uncertainty in the trend is estimated with an error budget approach and is below 3 mm/yr (at the 90% CL level[21]). Note that there is some difference between the coastal sea level trend and the sea level trend 25 km offshore. But this difference does not exceed 1.5 mm/yr (1 sigma value) over the satellite altimetry period (as shown by the difference between satellite altimetry and tide gauge records corrected for vertical land motion, see Wöppelmann and Marcos[41], or by the analysis from The Climate Change Initiative Coastal Sea Level Team[40]).

Glacial Isostatic Adjustment (GIA)

Local sea-level change due to glacial isostatic adjustment caused by ice loading and unloading are taken from the ICE-6G_C (VM5a) model[11]. Local land movement as response to deglaciation and combined with global topography and bathymetry to compute local sea-level change on a 0.2°x0.2° grid. This gridded dataset is projected to the DIVA coastal segments by assigning the average sea-level change value over all intersected grid cells to each segment.

Delta subsidence

Delta subsidence is estimated for 117 deltas, comprising the world's most significant deltas. For each delta a single indicative average value is assumed, except where stated otherwise, covering a similar time period to the sea-level measurements. For 40 of the more populated deltas, data is based on that developed by Ericson et al[13], with a few corrections. These include the Ganges-Brahmaputra delta where the value is taken from Brown and Nicholls[42], the Mekong delta from Erban et al[43] and Minderhoud et al[44], the North Italian Plain from Tos et al[45] and the Pearl River delta from Wang et al[46]. For the other 77 deltas, where there is little or no data, a minimum value of subsidence is assumed in all cases at 1 mm/yr, following the estimates of Meckel et al[47] . The delta extent is linked to the DIVA segments. Supplementary Table 1 summarises the deltas considered and subsidence values used.

Coastal city subsidence

The set of 136 coastal cities with more than one million people in 2005 as identified by Nicholls et al[34] and Hallegatte et al[48] are considered in this analysis, with two additional coastal cities within Indonesia which exceed the population threshold and are known to be subsiding: Semarang and Medan[49]. These large cities are considered in the analysis as they include the largest urban populations and the largest observed subsidence is reported in some of them as summarised in Supplementary Table 2. It is found that of these 138 cities, 36 cities are situated wholly or partly on deltaic/alluvial deposits which may subside due to subsurface fluid withdrawal and/or drainage. In each case, the additional subsidence beyond that captured in the delta subsidence estimates (Supplementary Table 1) is estimated based on a survey of the available literature or expert judgement if required. Given the wide range of values of subsidence reported, a low and a high estimate of average subsidence are made to represent the uncertainty. These are applied as indicative average estimates across the subsiding area in each city. These estimates of subsidence covering a similar time period to the sea-level measurements. The extent of subsidence in each city is defined by the extent of Holocene deposits, which in turn is linked to the DIVA segments (i.e., subsidence is not applied to the entire city unless this is appropriate). These estimates are designed to represent average subsidence values across the whole subsiding area within each city. Supplementary Table 2 summarises the coastal cites considered and the subsidence values used.

Socio-economic Scenarios

Population exposure is obtained by overlaying Shuttle Radar Topography Mission (SRTM) elevation data[50,51] with Global Rural-Urban Mapping Project (GRUMP) population data[52], using resampling methods[39]. As coastal urbanization trends play a major role in the population exposure analysis in this study, we use five regionalized population growth projections[39] based on the Shared Socio-economic Pathways (SSP2)[23,53-55]. As the population projections do not differ much until the middle of the 21st century, we only report the one based on the middle-of-the road scenario from the Shared Socio-economic Pathways (SSP2) in the main paper. Results for other population projections are shown in the Extended Data. We note that other population datasets would lead to different quantitative outputs as demonstrated in the analysis of Hinkel et al[31]. However, the main results in the article based on population weighting are unlikely to be sensitive to these differences as the relative distribution of population along the coast is common to all global population datasets.

In terms of population statistics, we consider the population living below the 10 m contour in 2015 for the population weighting of sea-level rise comprising 768 million people. To estimate population exposure to coastal flooding we also consider the coastal flood plain population living below the 100-year flood elevation which is dynamic in time due to relative sea-level change and population change. This population was 235 million people in 2015.

Mean and extreme sea-level rise scenarios to 2050

For SLR projections we use three global-mean SLR scenarios taken from Hinkel et al[31]: the 50th percentile of RCP2.6, RCP4.5 and RCP8.5 using the HadGEM-ES2 model[56]. Extreme water levels are assumed to uniformly increase with SLR, following 20th century observations[57]. Extreme water level distributions are taken from the GTSR database[58] and referenced to GeoID to be compatible with SRTM data[59].

Regional definitions utilised:

The 23 global coastal regions used in this study are defined by Future Earth Coast, formerly Land Ocean Interactions in the Coastal Zone (LOICZ), and are similar to earlier regional definitions[60,61]. These 23 regions divide the world's coast into geographical subsets, as defined in Supplementary Table 3.

Weighting Approach:

To compute global average values of the relative SLR components and their sums, the weighted average (*wrslr*) is computed as:

$$wrslr = \frac{\sum_{cls}\left(rslr(cls) * w(cls)\right)}{\sum_{cls} w(cls)} \qquad \text{Eq.1}$$

where *rslr(cls)* is the relative sea-level change in each coastline segment (*cls*).

For length-weighted global average we set *w(cls)* to the length of the coastline segment (*cls*). For population-weighted global average we set *w(cls)* to the population living in the Low Elevation Coastal Zone (i.e., the population living within 10-m elevation of mean sea level[62]) in each segment in 2015. In this analysis, the global coastal length totals 691,017 km and the global LECZ population is 768 million in 2015.

Coastal Flood Plain Population:

For the population in the flood plain we consider the 100-year flood plain (using water levels from Muis et al[58]) based on the elevation data from the SRTM and the population scenarios mentioned above. Changes with time are evaluated per segment assuming SLR (as defined above), $subsidence$ (or uplift) as defined above and population change (as defined above). Coastal adaptation including coastal defences are not considered, and the results simply reflect the flood plain population.

Studies before Muis et al[59] did not consider the difference in vertical datum of extreme sea levels and global land elevation and thus underestimated population exposure to flooding. While extreme water level datasets such as GTSR[59] use mean sea level as vertical datum, global elevation datasets, such as SRTM, are referenced to the EGM96 geoid[63]. The offset between mean sea level and the geoid can be up to 1.5 m, due to the dynamic sea surface of the ocean[64] and largely determined by ocean currents. Correcting the vertical datum increases the population exposed to the 100-year flood event by 39-60%[59].

As noted earlier, other population scenarios would lead to different quantitative estimates of coastal flood plain population (see Hinkel et al[31]), but the relative distribution of population along the coast would be similar. Hence, it would have little influence on the weighting by population described above.

Acknowledgments:

We thank Jason Ericson for sharing his dataset on delta subsidence.

Funding:

RJN was supported under the Deltas, vulnerability and Climate Change: Migration and Adaptation (DECCMA) project (IDRC 107642) under the Collaborative Adaptation Research Initiative in Africa and Asia (CARIAA) programme with financial support from the U.K. Government's Department for international Development (DFID) and the International Development Research Centre (IDRC), Canada and the PROTECT Project. The views expressed in this work are those of the creators and do not necessarily represent those of DFID and IDRC or their boards of governors. We thank the ESA CCI sea level project for providing the data and CNES for providing the data from Topex, Jason 1 2 and 3. Other portions of this research were made possible by support from the European Union through the projects RISES-AM (funded by the European Commission's Seventh Framework Programme, 2007 – 2013, under the grant agreement number 603396), GREEN-WIN and COACCH (funded by European Union's Horizon 2020 research and innovation programme under grant agreement No 642018 and No 776479, respectively). Further funding was received through to projects INSeaPTION and ISIpedia which are part of ERA4CS, an ERA-NET initiated by JPI Climate, and funded by FORMAS (SE), BMBF (DE, grant No 01LS1711C and No 01LS1703A), BMWFW (AT), IFD (DK), MINECO (ES), ANR (FR) with co-funding by the European Union (Grant 690462). This publication was supported by PROTECT. This project has received funding from the European Union's Horizon 2020 research and innovation programme under grant agreement No 869304, PROTECT contribution number 8.

Author contributions:

RJN, DL and JH designed and conducted the analysis and wrote the main paper. They also prepared the city subsidence and GIA data. SB and SH contributed to city subsidence data and prepared the data on delta subsidence. AT and JM prepared the socio-economic data. BM provided the satellite sea-level data and the expertise on climate-induced coastal sea-level rise. JF contributed to the city subsidence data from Asia, especially China. All authors read paper drafts and approved the final version.

Competing interests: "Authors declare no competing interests."

Data Availability Statement:

All datasets used in the production of this paper are available from http://doi.org/10.5281/zenodo.4434773. The sea-level data is referenced under the following

DOI: 10.5270/esa-sea_level_cci-1993_2015-v_2.0-201612 . It is freely available from http://www.esa-sealevel-cci.org/products

Computer Code Availability Statement:

The R code used to produce the numbers, tables and figures is available from http://doi.org/10.5281/zenodo.4434773

Correspondence and requests for materials should be addressed to Robert Nicholls

Robert.nicholls@uea.ac.uk

References:

30 Hinkel, J. *et al.* A global analysis of erosion of sandy beaches and sea-level rise: An application of DIVA. *Global and Planetary Change* **111**, 150-158, https://doi.org/10.1016/j.gloplacha.2013.09.002 (2013).

31 Hinkel, J. *et al.* Coastal flood damage and adaptation costs under 21st century sea-level rise. *Proceedings of the National Academy of Sciences* **111**, 3292, https://doi.org/10.1073/pnas.1222469111 (2014).

32 Schuerch, M. *et al.* Future response of global coastal wetlands to sea-level rise. *Nature* **561**, 231-234, https://doi.org/10.1038/s41586-018-0476-5 (2018).

33 Vafeidis, A. T. *et al.* A new global coastal database for impact and vulnerability analysis to sea-level rise. *Journal of Coastal Research* **24**, 917-924, (2008).

34 Nicholls, R. J. *et al.* Ranking port cities with high exposure and vulnerability to climate extremes - Exposure estimates. (OECD Publishing, Paris, France, 2008) https://doi.org/10.1787/011766488208

35 National Research Council. *Sea-level rise for the coasts of California, Oregon, and Washington: Past, present, and future*. (National Academic Press, 2012).

36 Ostanciaux, E., Husson, L., Choblet, G., Robin, C. & Pedoja, K. Present-day trends of vertical ground motion along the coast lines. *Earth-Science Reviews* **110**, 75-92, https://doi.org/10.1016/j.earscirev.2011.10.004 (2012).

37 Pfeffer, J. & Allemand, P. The key role of vertical land motions in coastal sea level variations: A global synthesis of multisatellite altimetry, tide gauge data and GPS measurements. *Earth and Planetary Science Letters* **439**, 39-47, https://doi.org/10.1016/j.epsl.2016.01.027 (2016).

38 Phien-wej, N., Giao, P. H. & Nutalaya, P. Land subsidence in Bangkok, Thailand. *Engineering Geology* **82**, 187-201, https://doi.org/10.1016/j.enggeo.2005.10.004 (2006).

39 Merkens, J.-L., Lincke, D., Hinkel, J., Brown, S. & Vafeidis, A. T. Regionalisation of population growth projections in coastal exposure analysis. *Climatic Change* **151**, 413-426, https://doi.org/10.1007/s10584-018-2334-8 (2018).

40 The Climate Change Initiative Coastal Sea Level Team *et al.* Coastal sea level anomalies and associated trends from Jason satellite altimetry over 2002–2018. *Scientific Data* **7**, https://doi.org/10.1038/s41597-020-00694-w (2020).

41 Wöppelmann, G. & Marcos, M. Vertical land motion as a key to understanding sea level change and variability. *Reviews of Geophysics* **54**, 64-92, https://doi.org/10.1002/2015RG000502 (2016).

42 Brown, S. & Nicholls, R. J. Subsidence and human influences in mega deltas: The case of the Ganges–Brahmaputra–Meghna. *Science of The Total Environment* **527-528**, 362-374, https://doi.org/10.1016/j.scitotenv.2015.04.124 (2015).

43 Erban, L. E., Gorelick, S. M. & Zebker, H. A. Groundwater extraction, land subsidence, and sea-level rise in the Mekong Delta, Vietnam. *Environmental Research Letters* **9**, 084010, https://doi.org/10.1088/1748-9326/9/8/084010 (2014).

44 Minderhoud, P. S. J. *et al.* Impacts of 25 years of groundwater extraction on subsidence in the Mekong delta, Vietnam. *Environmental Research Letters* **12**, 064006, https://doi.org/10.1088/1748-9326/aa7146 (2017).

45 Tos, L., Da Lio, C., Strozzi, T. & Teatini, P. Combining L- and X-Band SAR interferometry to assess ground displacements in heterogeneous coastal environments: The Po River Delta and Venice Lagoon, Italy. *Remote sensing* **8**, 308, https://doi.org/10.3390/rs8040308 (2016).

46 Wang, H. *et al.* InSAR reveals coastal subsidence in the Pearl River Delta, China. *Geophysical Journal International* **191**, 1119-1128, https://doi.org/https://doi.org/10.1111/j.1365-246X.2012.05687.x (2012).

47 Meckel, T. A., Ten Brink, U. S. & Williams, S. J. Sediment compaction rates and subsidence in deltaic plains: numerical constraints and stratigraphic influences. *Basin Research* **19**, 19-31, https://doi.org/10.1111/j.1365-2117.2006.00310.x (2007).

48 Hallegatte, S., Green, C., Nicholls, R. J. & Corfee-Morlot, J. Future flood losses in major coastal cities. *Nature Climate Change* **3**, 802-806, https://doi.org/10.1038/nclimate1979 (2013).

49 Chaussard, E., Amelung, F., Abidin, H. & Hong, S.-H. Sinking cities in Indonesia: ALOS PALSAR detects rapid subsidence due to groundwater and gas extraction. *Remote Sensing of Environment* **128**, 150-161, https://doi.org/10.1016/j.rse.2012.10.015 (2013).

50 Rabus, B., Eineder, M., Roth, A. & Bamler, R. The shuttle radar topography mission—a new class of digital elevation models acquired by spaceborne radar. *ISPRS Journal of Photogrammetry and Remote Sensing* **57**, 241-262, https://doi.org/10.1016/S0924-2716(02)00124-7 (2003).

51 Jarvis, A., Reuter, H. I., Nelson, A. & Guevara, E. Hole-filled SRTM for the globe Version 4. (2008) http://srtm.csi.cgiar.org.

52 Center for International Earth Science Information Network - CIESIN - Columbia University, International Food Policy Research Institute - IFPRI, The World Bank & Centro Internacional de Agricultura Tropical - CIAT. *Global Rural-Urban Mapping*

Project, Version 1 (GRUMPv1): Population Count Grid. (NASA Socioeconomic Data and Applications Center (SEDAC), 2011). https://doi.org/10.7927/H4VT1Q1H.

53 IIASA. SSP Database. (2012) https://tntcat.iiasa.ac.at/SspDb.

54 O'Neill, B. C. *et al.* A new scenario framework for climate change research: the concept of shared socioeconomic pathways. *Climatic Change* **122**, 387-400, https://doi.org/10.1007/s10584-013-0905-2 (2014).

55 Samir, K. C. & Lutz, W. The human core of the shared socioeconomic pathways: Population scenarios by age, sex and level of education for all countries to 2100. *Global Environmental Change* **42**, 181-192, https://doi.org/10.1016/j.gloenvcha.2014.06.004 (2017).

56 Collins, W. J. *et al.* Development and evaluation of an Earth-System model – HadGEM2. *Geoscientific Model Development* **4**, 1051-1075, https://doi.org/10.5194/gmd-4-1051-2011 (2011).

57 Menéndez, M. & Woodworth, P. L. Changes in extreme high water levels based on a quasi-global tide-gauge data set. *Journal of Geophysical Research: Oceans* **115**, https://doi.org/10.1029/2009JC005997 (2010).

58 Muis, S., Verlaan, M., Winsemius, H. C., Aerts, J. C. J. H. & Ward, P. J. A global reanalysis of storm surges and extreme sea levels. *Nature Communications* **7**, 11969, https://doi.org/10.1038/ncomms11969 (2016).

59 Muis, S. *et al.* A comparison of two global datasets of extreme sea levels and resulting flood exposure. *Earth's Future* **5**, 379-392, https://doi.org/10.1002/2016EF000430 (2017).

60 Hoozemans, F. M. J., Marchand, M. & Pennekamp, H. A. Sea level rise: A global vulnerability analysis: Vulnerability assessment for population, coastal wetlands and rice production on a global scale. (Delft Hydraulics, the Netherlands, 1993) https://repository.tudelft.nl/islandora/object/uuid:651e894a-9ac6-49bf-b4ca-9aedef51546f.

61 Nicholls, R. J. & Hoozemans, F. M. J. in *Encyclopedia of Coastal Science* (ed Maurice L. Schwartz) Ch. Global vulnerability analysis, 486-491 (Springer Netherlands, 2005) https://doi.org/10.1007/1-4020-3880-1_155

62 McGranahan, G., Balk, D. & Anderson, B. The rising tide: assessing the risks of climate change and human settlements in low elevation coastal zones. *Environment and Urbanization* **19**, 17-37, https://doi.org/10.1177/0956247807076960 (2007).

63 Farr, T. G. *et al.* The Shuttle Radar Topography Mission. *Reviews of Geophysics* **45**, https://doi.org/https://doi.org/10.1029/2005RG000183 (2007).

64 Schaeffer, M., Hare, W., Rahmstorf, S. & Vermeer, M. Long-term sea-level rise implied by 1.5 °C and 2 °C warming levels. *Nature Climate Change* **2**, 867-870, https://doi.org/10.1038/nclimate1584 (2012).

65 Becker, M. *et al.* Water level changes, subsidence, and sea level rise in the Ganges–Brahmaputra–Meghna delta. *Proceedings of the National Academy of Sciences* **117**, 1867, https://doi.org/10.1073/pnas.1912921117 (2020).

66 Higgins, S. A. *Measurements of deltas at risk* (University of Colorado, Boulder, Colorado, USA, 2014).

67 Wöppelmann, G. *et al.* Is land subsidence increasing the exposure to sea level rise in Alexandria, Egypt? *Geophysical Research Letters* **40**, 2953-2957, https://doi.org/10.1002/grl.50568 (2013).

68 Gebremichael, E. *et al.* Assessing land deformation and sea encroachment in the Nile Delta: A radar interferometric and inundation modeling approach. *Journal of Geophysical Research: Solid Earth* **123**, 3208-3224, https://doi.org/10.1002/2017JB015084 (2018).

69 Deltacommissie. Working together with water. A living land builds for its future. (2008) http://www.deltacommissie.com/en/advies.

70 Suanez, S. & Provansal, M. Morphosedimentary behaviour of the deltaic fringe in comparison to the relative sea-level rise on the Rhone delta. *Quaternary Science Reviews* **15**, 811-818, https://doi.org/10.1016/S0277-3791(96)00067-4 (1996).

71 Samsonov, S. V. *et al.* Rapidly accelerating subsidence in the Greater Vancouver region from two decades of ERS-ENVISAT-RADARSAT-2 DInSAR measurements. *Remote Sensing of Environment* **143**, 180-191, https://doi.org/10.1016/j.rse.2013.12.017 (2014).

72 Mazzotti, S., Lambert, A., Van der Kooij, M. & Mainville, A. Impact of anthropogenic subsidence on relative sea-level rise in the Fraser River delta. *Geology* **37**, 771-774, https://doi.org/10.1130/g25640a.1 (2009).

73 Zhao, J. K., Wu, M. J., Liu, S. X. & Shen, H. Z. The relation between groundwater exploitation and land subsidence in the coast plain of Zhejiang Province (in Chinese). *Geological Journal of China Universities* **12**, 185-194, (2006).

74 Xu, N. Z., Jiang, Y. H., Wang, J. D., Liu, H. & Jia, J. The types and characteristics of the ground subsidence in southeastern China coastal region (in Chinese). *Journal of Catastrophology* **20**, 67-72, (2005).

75 Xue, Y.-Q., Zhang, Y., Ye, S.-J., Wu, J.-C. & Li, Q.-F. Land subsidence in China. *Environmental Geology* **48**, 713-720, https://doi.org/10.1007/s00254-005-0010-6 (2005).

76 Yang, C., Pan, L. Y. & Yu, C. Land subsidence control in Wenzhou, Zhejiang (in Chinese). *Low Temperature Architecture Technology* **158**, 114-115, (2011).

77 Orejarena-Rondón, A. F. *et al.* Coastal impacts driven by sea-level rise in Cartagena de Indias. *Frontiers in Marine Science* **6**, https://doi.org/10.3389/fmars.2019.00614 (2019).

78 Chatterjee, R. S. *et al.* Subsidence of Kolkata (Calcutta) City, India during the 1990s as observed from space by Differential Synthetic Aperture Radar Interferometry (D-InSAR) technique. *Remote Sensing of Environment* **102**, 176-185, https://doi.org/10.1016/j.rse.2006.02.006 (2006).

79 Sahu, P. & Sikdar, P. K. Threat of land subsidence in and around Kolkata City and East Kolkata Wetlands, West Bengal, India. *Journal of Earth System Science* **120**, 435-446, https://doi.org/10.1007/s12040-011-0077-2 (2011).

80 Abidin, H. Z., Andreas, H., Gumilar, I., Sidiq, T. P. & Fukuda, Y. Land subsidence in coastal city of Semarang (Indonesia): characteristics, impacts and causes. *Geomatics, Natural Hazards and Risk* **4**, 226-240, https://doi.org/10.1080/19475705.2012.692336 (2013).

81 Deltares. *Sinking cities: An integrated approach towards solutions*. (Deltares, 2014).

82 Kasmarek, M. C., Gabrysch, R. K. & Johnson, M. R. Estimated land-surface subsidence in Harris County, Texas, 1915-17 to 2001. Report No. 3097, (Reston, VA, 2009) http://pubs.er.usgs.gov/publication/sim3097. https://doi.org/10.3133/sim3097

83 Dixon, T. H. *et al.* Subsidence and flooding in New Orleans. *Nature* **441**, 587-588, https://doi.org/10.1038/441587a (2006).
84 Nguyen, Q. T. The main causes of land subsidence in Ho Chi Minh City. *Procedia Engineering* **142**, 334-341, https://doi.org/10.1016/j.proeng.2016.02.058 (2016).
85 Nicholls, R. J. *et al.* A global analysis of subsidence, relative sea-level change and coastal flood exposure. Dataset. http://doi.org/10.5281/zenodo.4434773 (2021).

List of Tables

Table 1: Contribution of the climate and geological components to relative sea-level change for length-weighted and population-weighted cases, respectively. Average values are reported, except for cities and the global-mean sum where a low/high range is used to express the uncertainty in subsidence (see Supplementary Table 2).

List of Figures

Fig 1: Cumulative distribution of contemporary length-weighted and population-weighted coastal relative sea-level rise, respectively. This includes lower and upper estimates to express uncertainty, although for length weighting the difference is too small to be seen.

Fig 2: Average relative sea-level rise for 23 coastal world regions. (a) Length-weighted and (b) population-weighted. (see Supplementary Table 3 for region definitions).

Fig 3: Global population in the coastal flood plain from 2015 to 2050. This considers sea-level rise scenarios under RCP2.6, RCP4.5 and RCP8.5 emissions, as well as no climate-induced sea-level rise as a reference, and assumes the SSP2 socio-economic scenario. Subsidence/GIA assumptions as indicated. (a) No vertical land movement. (b) GIA only. (c) GIA and delta subsidence. (d) GIA, delta and uncontrolled city subsidence. (e) GIA, delta and city subsidence controlled to 5 mm/yr. The uncertainty bands reflect uncertainty in rates of city subsidence (see Fig. 1). Simulations start in 1995, while the flood plain is defined based on the 100-year event.

List of Extended Data Figures

Extended Data Fig 1: Cumulative distribution of contemporary coastal relative SLR. (a) length-weighted, (b) population-weighted. Each panel shows climate-induced SLR alone, and then progressively adds the other components comprising: (1) GIA, (2) GIA and delta subsidence combined, and (3) GIA, delta subsidence and uncontrolled city subsidence combined. For uncontrolled city subsidence, the uncertainty is considered by using a low and high estimate. For length weighting, the main change occurs due to adding the GIA component, which reduces the median and mean SLR. Considering delta and city subsidence has little effect as only 6.5 percent and 0.8 percent of the world's coast length are affected. For population weightings, adding GIA also has an effect, but it is smaller than for length weighting being -0.3 mm/yr on mean SLR. This reflects that the coastal population is preferentially located in areas where GIA causes subsidence, which counters the effect GIA has when considering length weighting. Adding delta and then uncontrolled city subsidence has a significant effect reflecting the large populations in these areas. In the median, these two components add 1.19 mm/yr and an additional 0.62 mm/yr of SLR rise, respectively. The asymmetric distribution of the high-end tail leads to a larger effect on the mean SLR at 1.6 mm/yr due to delta subsidence alone, and an additional 2.7 to 4.8 mm/yr due to city subsidence alone (Table 1).

Extended Data Fig 2: Sea-level rise components versus coastal population density for all the coastal segments considered in the analysis. These comprise (a) climate-induced sea-level rise only, (b) GIA only, (c) high estimates of uncontrolled city subsidence only, (d) delta subsidence only, and (e) the sum of all four components considered previously. The linear best fit and the explained variance are shown in each case. While the explained variance with such a linear fit is small, the slopes are significantly different from zero in all cases.

Extended Data Fig 3: Global total of people living in the coastal flood plain from 2015 to 2050 under a range of socio-economic and climate scenarios. These comprise five different SSP-based regionalised population scenarios (SSP1 to SSP5), and no climate-induced SLR and the RCP2.6 and RCP8.5 SLR scenarios, respectively. Assumptions concerning geological components of relative SLR are as follows: Column (a) No geological component, Column (b) GIA only, Column (c) GIA and delta subsidence, Column (d) GIA, delta and uncontrolled city subsidence. Column (e) GIA, delta and controlled city subsidence (to a maximum of 5 mm/yr). The uncertainty bands in (d) reflect uncertainty in the rates of city subsidence (see Fig 1). All simulations start in 1995. The results indicate little variation between SSPs to 2050.

List of Supplementary Tables

Supplementary Table 1: Subsidence rates applied by delta: a positive value indicates subsidence and a negative value indicated aggradation. Expert judgement draws on Meckel et al[47].

Supplementary Table 2: Additional subsidence rates applied by city: a positive value indicates subsidence. If cities are not listed here, no additional subsidence is applied.

Supplementary Table 3: Regional definitions as used in Fig 2.

Supplementary Table 4: Regional-mean relative sea-level rise comparing length and population weightings. Rows coloured yellow see a 50 to 100% increase, while rows coloured green see more than 100% increase moving from length to population weightings, respectively. In the other rows, changes are within +50%.

Extended Data Figures

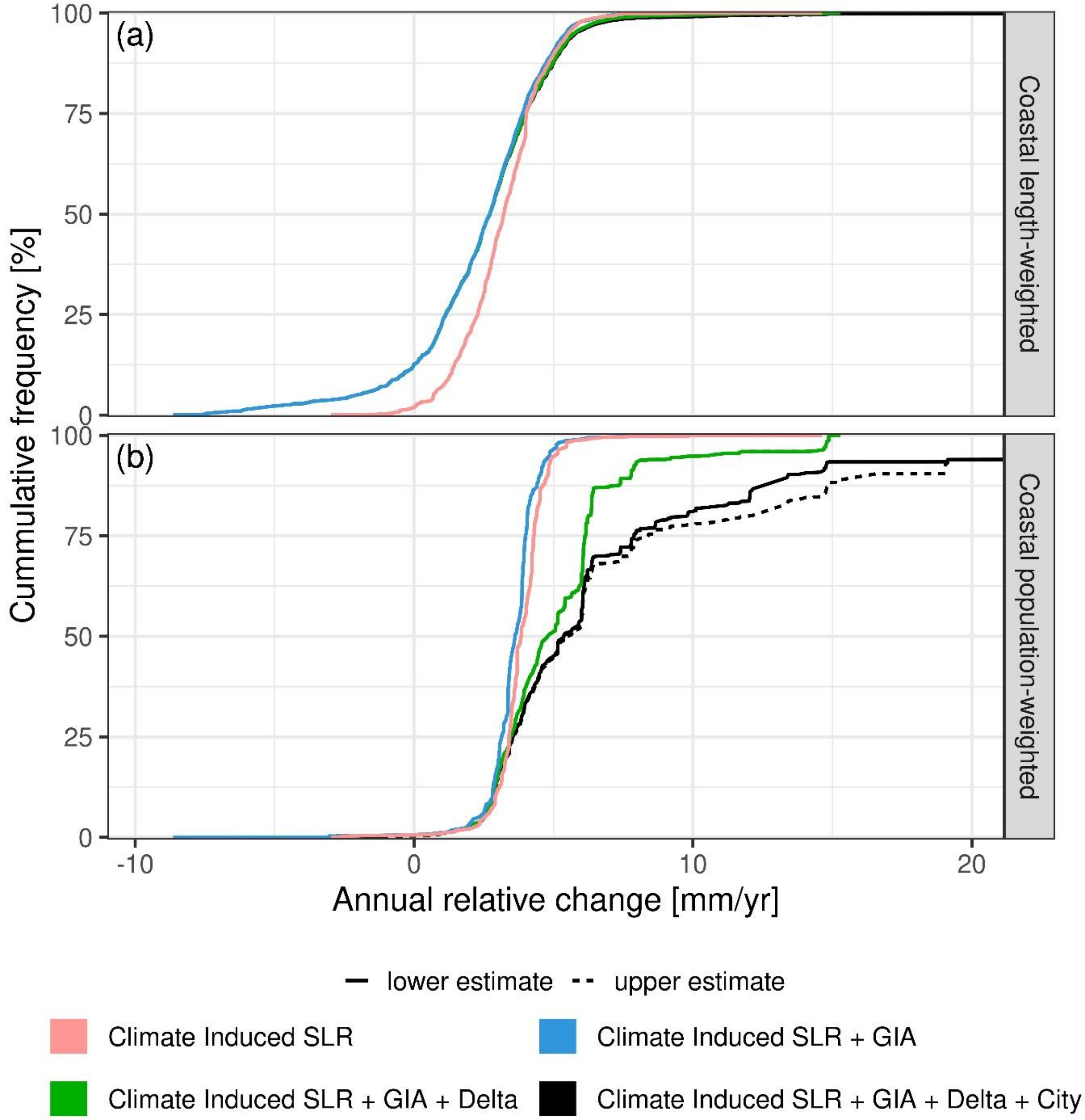

***Extended Data Fig 1**: Cumulative distribution of contemporary coastal relative SLR. (a) length-weighted, (b) population-weighted. Each panel shows climate-induced SLR alone, and then progressively adds the other components comprising: (1) GIA, (2) GIA and delta subsidence combined, and (3) GIA, delta subsidence and uncontrolled city subsidence combined. For uncontrolled city subsidence, the uncertainty is considered by using a low and high estimate.*

For length weighting, the main change occurs due to adding the GIA component, which reduces the median and mean SLR. Considering delta and city subsidence has little effect as only 6.5 percent and 0.8 percent of the world's coast length are affected. For population weightings, adding GIA also has an effect, but it is *smaller than for length weighting being -0.3 mm/yr on mean SLR. This reflects that the coastal population is preferentially located in areas where GIA causes subsidence, which counters the effect GIA has when considering length weighting. Adding delta and then uncontrolled city subsidence has a significant effect reflecting the large populations in these areas. In the median, these two components add 1.19 mm/yr and an additional 0.62 mm/yr of SLR rise, respectively. The asymmetric distribution of the high-end tail leads to a larger effect on the mean SLR at 1.6 mm/yr due to delta subsidence alone, and an additional 2.7 to 4.8 mm/yr due to city subsidence alone (Table 1).*

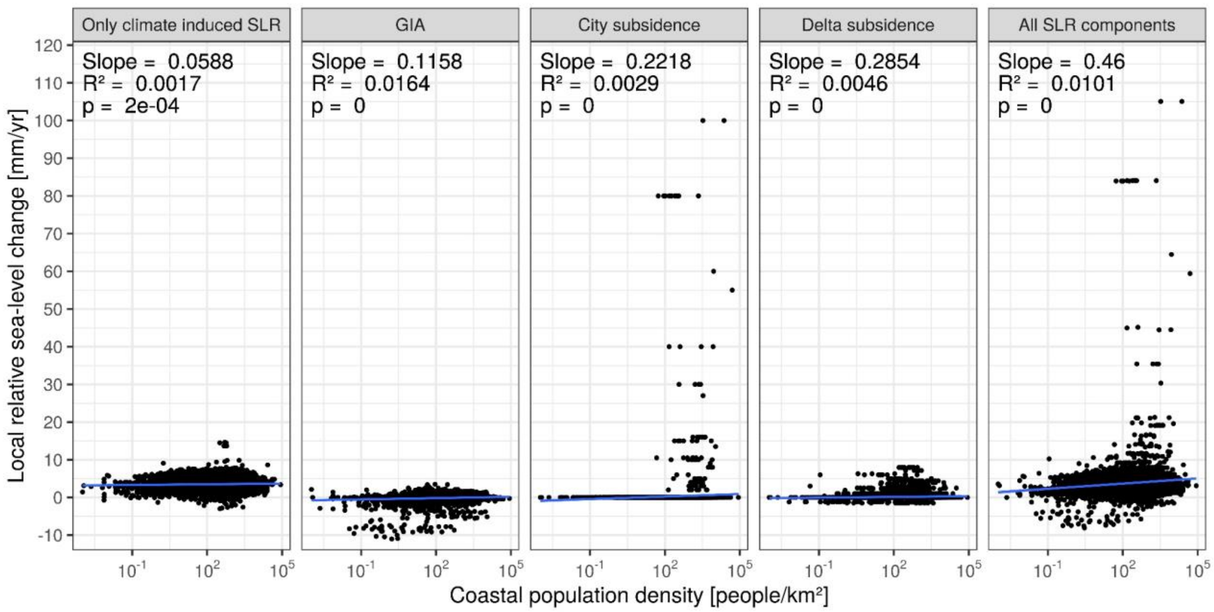

Extended Data Fig 2: *Sea-level rise components versus coastal population density for all the coastal segments considered in the analysis. These comprise (a) climate-induced sea-level rise only, (b) GIA only, (c) high estimates of uncontrolled city subsidence only, (d) delta subsidence only, and (e) the sum of all four components considered previously. The linear best fit and the explained variance are shown in each case. While the explained variance with such a linear fit is small, the slopes are significantly different from zero in all cases.*

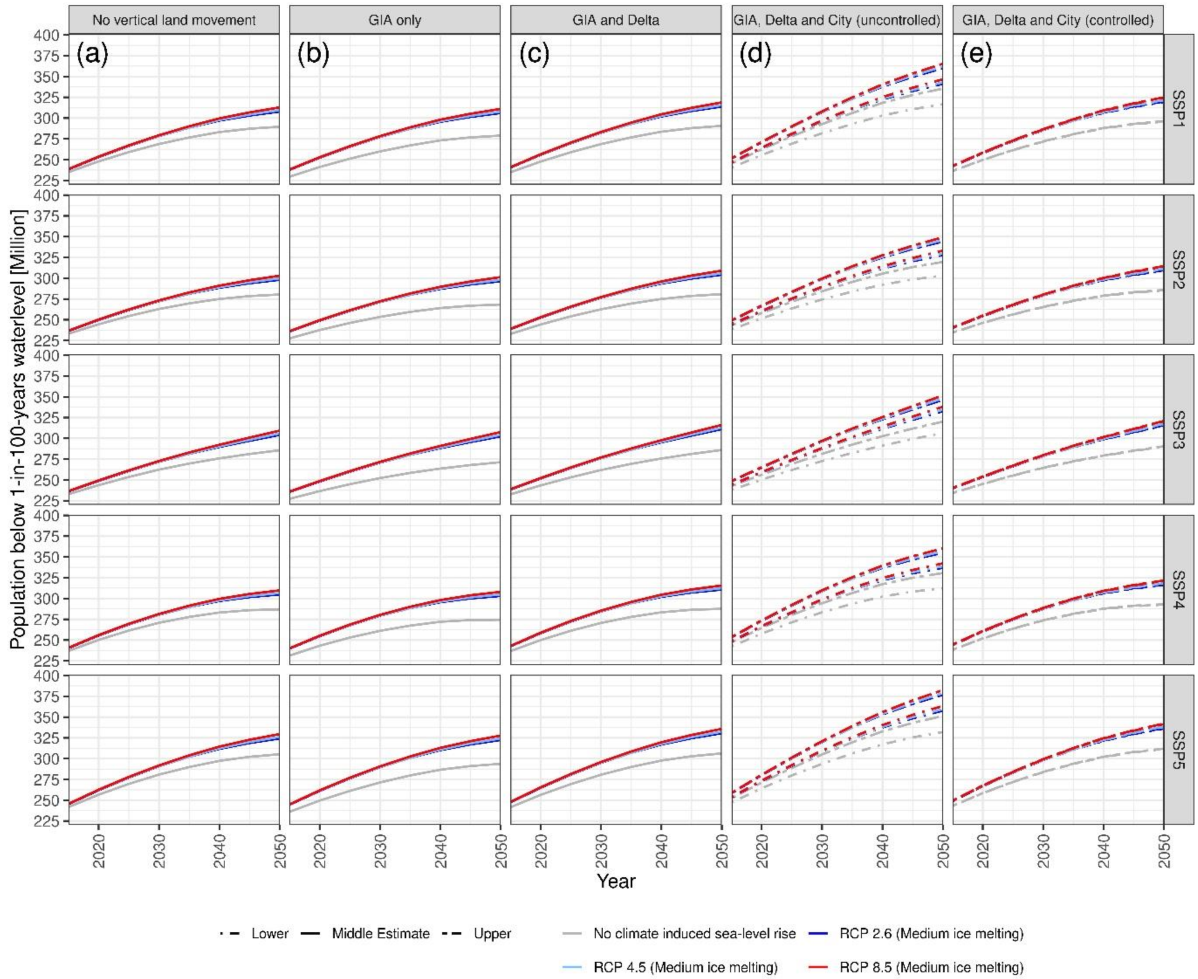

Extended Data Fig 3: *Global total of people living in the coastal flood plain from 2015 to 2050 under a range of socio-economic and climate scenarios. These comprise five different SSP-based regionalised population scenarios (SSP1 to SSP5), and no climate-induced SLR and the RCP2.6 and RCP8.5 SLR scenarios, respectively. Assumptions concerning geological components of relative SLR are as follows: Column (a) No geological component, Column (b) GIA only, Column (c) GIA and delta subsidence, Column (d) GIA, delta and uncontrolled city subsidence. Column (e) GIA, delta and controlled city subsidence (to a maximum of 5 mm/yr). The uncertainty bands in (d) reflect uncertainty in the rates of city subsidence (see Fig 1). All simulations start in 1995. The results indicate little variation between SSPs to 2050.*